Coronary arterial tree remodeling in right ventricular hypertrophy

GHASSAN S. KASSAB, KIYOTAKA IMOTO, FRANCIS C. WHITE, CARMELA A. RIDER, YUAN-CHENG B. FUNG, AND COLIN M. BLOOR
Department of Applied Mechanics and Engineering Sciences/Bioengineering, Institute for Biomedical Engineering, and Department of Pathology, University of California, San Diego, La Jolla, California 92093-0412; and Department of Surgery, Yokohama City University School of Medicine, Yokohama 236, Japan.

Kassab, Ghassan S., Kiyotaka Imoto, Francis C. White, Carmela A. Rider, Yuan-Cheng B. Fung, and Colin M. Bloor. Coronary arterial tree remodeling in right ventricular hypertrophy. *Am. J. Physiol.* 265 (*Heart Circ. Physiol.* 34): H366–H375, 1993.—We investigated coronary vascular adaptations occurring in right ventricular hypertrophy (RVH). Six pigs had RVH induced by pulmonary artery stenosis for 5 wk. Three pigs served as controls. At autopsy we made silicone elastomer casts of the right coronary arteries (RCA) and collected morphometric data. We organized the segments and their diameters and lengths into a framework of a modified Strahler's ordering scheme in which the order number of an offspring is increased only if its diameter is greater than the diameters of its parents by a specific amount. The segments of the same order arranged in series are combined into elements. In RVH the total number of orders of vessels was larger than the control by 1; the total number of elements in each order increased greatly, whereas the diameters and lengths of each order decreased somewhat. The total RCA resistance decreased in RVH mainly because the total cross-sectional area (CSA) of every order was increased. Because the diameters of the resistance vessels decreased, this decrease in total RCA resistance was due to a numerical increase in resistance vessels. These findings indicate that new flow channels have been established. In contrast, the RCA was remodeled in that the lumen diameter increased. Pressure-flow curves showed a decrease of coronary resistance in RVH, in agreement with the morphometric findings. We conclude that there is significant remodeling of the coronary arterial vasculature in RVH, and any future analysis of coronary hemodynamics of the right ventricle in hypertrophy must take the morphometric remodeling into account.

vascular remodeling; morphometry; silicone elastomer; diameter-defined Strahler system

PRESSURE-OVERLOAD CARDIAC HYPERTROPHY induces adaptive changes in both the left and right ventricles. These changes include the enlargement of myocytes (1, 4, 6, 24) and, in left ventricular hypertrophy (LVH), a decrease in the total number of arterial vessels per unit volume, which results in a loss of coronary blood flow reserve (3–7, 9, 21, 23, 29, 33, 34). Whether right ventricular hypertrophy (RVH) induces a similar decrease in vascularity and a relative underperfusion was unknown prior to our investigation. Some studies suggest that an increase in right ventricular mass does not induce severe functional changes (5, 10, 17, 19, 20, 24). However, there is evidence that vascular growth occurs in pressure-overload RVH (1, 5, 10, 12, 17, 19, 20, 24, 32). Recently, there has been some attempt to quantify the vascular remodeling in LVH (1, 27, 30). However, morphological data of vascular growth in RVH are lacking except for the study by White et al. (32), in which they measured the diameter and number density (number/mm^2) of capillaries, the diameter and number density of 10- to 25-μm vessels, and the density of 25- to 100-μm vessels in normal and RVH hearts. Although these data are useful, they do not allow for hemodynamic analysis of blood flow in the heart; i.e., alone, these data are insufficient to calculate the change of vascular resistance from the normal to the hypertrophic right ventricle.

The relationship between coronary pressure and flow in the right ventricle and the amount of blood flow per unit mass of myocardium are important to the understanding of the heart. Any rational approach to coronary hemodynamics would require morphometric data of the coronary vasculature, including the branching pattern, and the diameter, length, and number of parallel elements in each generation of vessels. To understand the function of a hypertrophic ventricle one must know the blood flow in the myocardium and the changes that occur in the coronary vasculature.

In this study we examine the morphometric aspects of the vascular remodeling in RVH. Detailed morphometric techniques are used to describe changes in the branching pattern, diameters, lengths, and numbers of vessels of every order of the right ventricular branches, including the change of the total number of orders. In turn, these data are used to calculate the total CSA of the coronary vasculature of successive orders of arteries. The morphometric data characterize quantitatively the growth of the coronary vasculature in progressive RVH.

METHODS

Animal preparation. Nine Duroc farm pigs were used in this study. Three of these animals were used as controls and six had RVH induced by a stenosis of the pulmonary artery. Surgical anesthesia was induced with ketamine hydrochloride (25 mg/kg im) and thiamylal sodium (20 mg/kg iv). Animals were maintained on surgical anesthesia with halothane (1–2%) and oxygen. Lidocaine (80 mg iv) was administered as a bolus before cardiac instrumentation. A left lateral fourth-intercostal-space thoracotomy was performed using sterile techniques. A fluid-filled Silastic pressure-monitoring catheter was placed in a jugular vein and advanced into the right atrium and right ventricle. Right atrial and right ventricular pressures were measured on a Hewlett-Packard chart recorder (model 5912A, Palo Alto, CA). A Silastic snare stenosed the pulmonary artery until the right ventricular systolic pressures were raised to 9.3–10.7 kPa (70–80 mmHg). The snare was then fixed to maintain this degree of stenosis. The thoracotomy was closed, and the animals were allowed to recover for 5 wk, during which time the right ventricular pressure was hypertensive and the muscle hypertrophied.

The control and the hypertrophic pigs of the same age (4 mo)

and weight (31 ± 2 kg) were then prepared for morphometric study. Each animal was anesthetized as described in the above protocol, intubated, and ventilated with room air using a Harvard mechanical respirator. A midline sternotomy was performed, and the aorta was cannulated. Arterial pressure was monitored via a carotid artery; right ventricular pressure was measured at the termination of the study by inserting a catheter into the right ventricle via the jugular vein. KCl was given to arrest the heart, and then we perfused the heart with a cardioplegic solution, as previously described (16). The right coronary artery (RCA) was cannulated, whereas the left anterior descending coronary artery (LAD) and left circumflex coronary artery (LCX) were ligated.

Determination of pressure-flow relationship of RCA artery. To compare the resistances to blood flow of the control and hypertrophic right ventricles we determined the pressure-flow (P-$\dot{Q}$) relationships in these hearts with the setup shown in Fig. 1. A rigid tube with a lumen diameter of 0.14 cm and a length of 98 cm was used to perfuse the RCA and served as a flowmeter in the interim. For the flows used in these experiments, the maximum Reynolds number was <400, so the effect of turbulence was negligible. In calibrating the tube as a flowmeter, the inlet and outlet pressures were measured with pressure transducers on a Hewlett-Packard strip-chart recorder while the flows were measured by collecting the volumes of flow in a graduated cylinder for a given period of time. The fluid used to measure the P-$\dot{Q}$ curve of the RCA was the cardioplegic solution described previously (16). Figure 1 shows how the rigid tube was incorporated into our isolated heart preparation (stopcock closed to *tube 1* and opened to *tube 2*). In the RCA experiments, the pressure changes were imposed with a regulator according to selected loading and unloading ramps. The pressures P_1 and P_2 were recorded on a Hewlett-Packard strip-chart recorder. Flows were calculated from the pressure differences, $P_1 - P_2$, according to the calibrated tube flow resistance. The inlet pressure to the RCA is P_2 minus a small pressure drop correction for the 12-cm-long cannulating catheter with a diameter of, for example, 0.14 cm. The pressure difference across the right ventricle circuit was P_2 minus the outlet venous pressure, which was zero or atmospheric. The RCA was preconditioned with several loading and unloading cycles before recording the final data. In this way, the RCA P-$\dot{Q}$ curve was obtained.

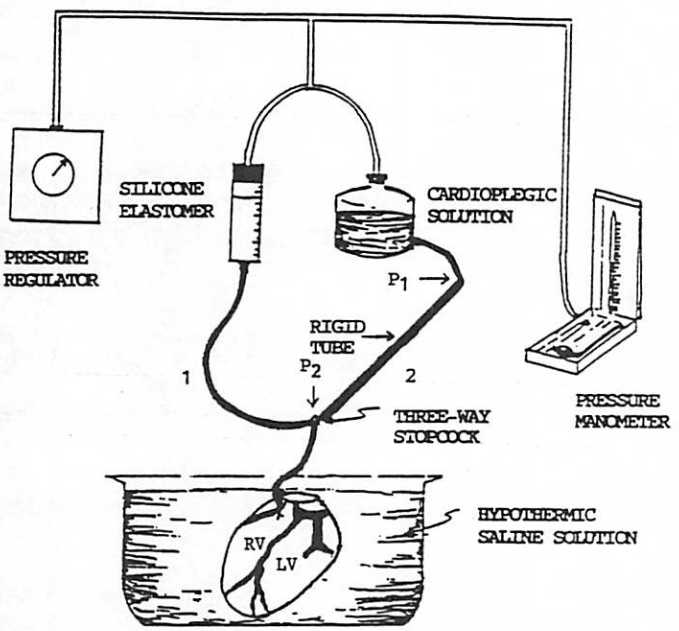

Fig. 1. Schematic diagram of perfusion apparatus. RV and LV, right and left ventricles, respectively; *1* and *2* are *tubes 1* and 2; P_1 and P_2 are inlet and outlet pressures of the rigid tube, respectively.

Determination of myocardial region perfused by RCA ventricular branches. Our morphometric data were measured from polymer casts of the RCA vasculature, which was perfused with a silicone elastomer (CP-101, Flow Technology), catalyzed with 6.2% stannous 2-ethylhexoate and 3.1% ethyl silicate in a liquid state under controlled pressures and then allowed to solidify in a specific period of time at a static pressure of 80 mmHg. The protocol for casting the RCA was identical to that described previously (16).

In this study, we were interested in the morphometry of the normal and hypertrophied RCA branches that supply the right ventricle. Hence we dissected the RCA cast to identify the atrial branches and tied a suture around every atrial branch before corrosion of the myocardium. A suture was also tied around the posterior descending artery (RCA-PDA) that supplies the posterior interventricular septum and posterior portions of the left ventricle. Only the right ventricular branches (RCA-RVB) were measured in the morphometric analysis. The two atria were cut away from the casted heart at the level of the atrioventricular valves. The right ventricular free wall was then excised and weighed. The left ventricle (including the septum) was also weighed. However, the right ventricular free wall mass is greater than the myocardial mass supplied by the RCA-RVB, since some branches of the LAD and LCX supply the posterior right ventricular wall. Because the LAD and LCX arteries were not perfused with elastomer, a border was found between the elastomer-perfused and nonperfused right ventricular myocardium. This was determined by removing myocardial plugs along the border, sectioning, clearing, and viewing them under the microscope. Hence the region perfused by RCA-RVB was measured.

Histological and cast studies of RCA ventricular branches. For histological studies of smaller coronary arteries of orders 1–4, 12 plugs of myocardial tissue were removed from the right ventricles of 3 RVH pigs and 8 plugs from the right ventricles of 2 control pigs. Each transmural plug was ~4 × 4 mm in cross section and extended from epicardium to endocardium. The method of preparation of histological sections was identical to that described previously (16). Figure 2 shows an example of a cleared histological section taken 4.7 mm from the epicardial surface of a hypertrophic right ventricle.

For cast studies, the same hearts used for the histological studies of the microvasculature were corroded after removal of tissue plugs for histological sections. We corroded the tissue with a 30% KOH solution for several days. The corroded tissue was washed away with soap and water. The veins were carefully pruned away, leaving the RCA and its branches intact with clusters of capillaries. The casts of RCA beds in normal and hypertrophic right ventricles are shown in Fig. 3.

Using methods developed in the earlier study of Kassab et al. (16), we measured the arterial trees from histological specimens of the right ventricular free wall and the right ventricular branches from the polymer casts of the RCA. We assigned order numbers to arterial vessels in histological specimens and corroded casts according to the diameter-defined Strahler system described by Kassab et al. (16) and measured the diameters and lengths, combined segments of the same order but connected in series into elements, counted the number of elements in each order, and obtained their connectivity matrices.

Mathematical description of branching pattern, order number, and connectivity matrix. To better describe the branching pattern of the arteries in RVH, we introduced three innovations in a companion study (16). In brief, a diameter-defined Strahler system is used, whereby capillaries are defined as vessels of order 0. The smallest arteries (arterioles) are identified as vessels of order 1. Arterioles are identified by their tortuosity, and capillaries are identified by their nontreelike topology (15). Two

Fig. 2. Photomicrograph of arterioles (a) in hypertrophic pig RV. This 70-μm-thick section taken ~4.7 mm from epicardial surface shows several arterioles feeding a capillary bed and a nearby venule (v) draining it.

order 1 vessels meet to form a vessel of order 2, if its diameter is larger than that of the order 1 vessels by a certain amount; or remain at order 1, if the new diameter is not large enough. Two order 2 vessels meet to yield a vessel of order 3, if the diameter criterion is satisfied; or remain at order 2, if the diameter is not large enough, and so on. The diameter criterion is the dividing line between vessels of order n and vessels of order $n + 1$

$$[(D_{n-1} + \Delta_{n-1}) + (D_n - \Delta_n)]/2 \quad (1)$$

on the left, and

$$[(D_n + \Delta_n) + (D_{n+1} - \Delta_{n+1})]/2$$

on the right, where D_n is the mean diameter of vessels of order n, and Δ_n is the standard deviation of the diameters of vessels of order n. This definition eliminates the overlap of histograms of diameters of all vessels in successive orders and enables an accurate analog circuit to be constructed for hemodynamics. The second innovation is to combine all vessel segments of a given order but connected in series into elements. The third innovation is to describe asymmetric branching by a connectivity matrix, $\mathbf{C}(m,n)$, whose element in row m and column n is the ratio of the total number of elements of order m that arise directly from parent elements of order n divided by the total number of elements of order n.

RESULTS

We induced RVH by stenosis of the pulmonary artery for 5 wk. The mean and peak systolic pressures of the right ventricle increased to three to four times the control levels. The right ventricle-to-left ventricle weight ratio doubled over the 5 wk.

Table 1 summarizes the heart weights, blood pressures, and morphometric measurements of the two control and three hypertrophic right ventricles. Morphometric measurements were made on all histological specimens from all five right ventricles. We conducted completely detailed polymer-cast measurements on one control right ventricle and one hypertrophic right ventricle. We examined the variability between the two control hearts and the three hypertrophic hearts by analyzing the morphometric data from each heart separately. The morphometric data from the two control hearts were similar, as were the data from the three hypertrophic hearts. Hence the morphometric data for the two control hearts were combined. Likewise, the morphometric data from the three hypertrophic hearts for each respective order were combined before conducting the statistical analysis shown in Tables 2–6.

The P-$\dot{Q}$ relation of the rigid tube used as a flowmeter was fitted by the method of least squares. The result is

$$\text{Pressure drop (mmHg)} = 417\ (\text{mmHg}\cdot\text{ml}^{-1}\cdot\text{s}^{-1}) \times \text{flow (ml/s)} - 0.512\ (\text{mmHg}) \quad (2)$$

with a correlation coefficient of 0.999. Figure 4 shows the P-$\dot{Q}$ relationship of the RCA. The two curves for each

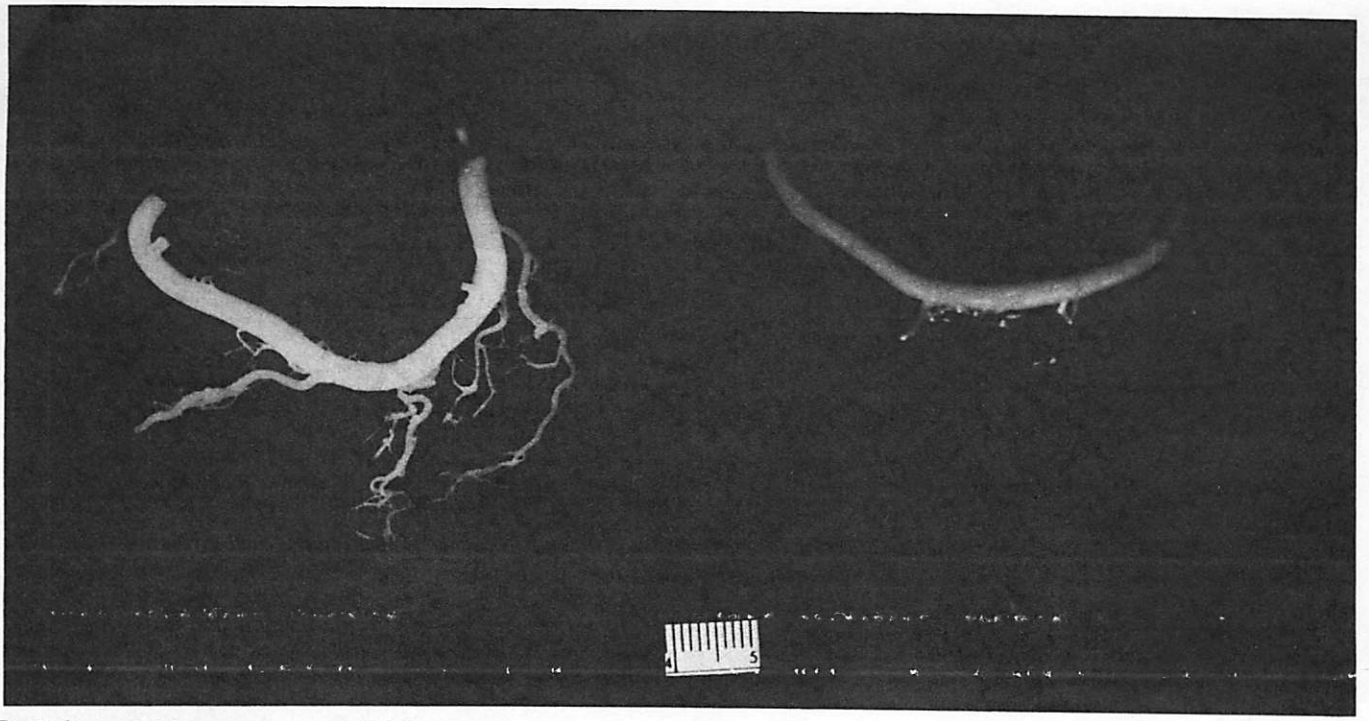

Fig. 3. Casts of right coronary artery (RCA) in control (*left*) and hypertrophic (*right*) pig RV. Atrial branches and posterior descending artery were excised.

heart correspond to loading and unloading of pressure and were fitted with second-order polynomials by the least-squares method.

The RCA and RCA-RVB arteries of control and hypertrophic right ventricles are shown in Fig. 5. The average diameters and lengths of the vessel segments are marked. For the trunk of the RCA, excluding the RCA-PDA, the average diameters and lengths were 2,469 ± 242 and 2,988 ± 1,689 μm, respectively, in the control right ventricle (N = 16 vessel segments) and 2,926 ± 320 and 3,484 ± 1,641 μm, respectively, in the hypertrophic right ventricle (N = 22 vessel segments). The total lengths of the RCA trunk with segments in series as an element, excluding the RCA-PDA, were 47.8 mm in the control right ventricle and 76.7 mm in the hypertrophic right ventricle. A total of 16 subtrees, i.e., RCA-RVB arisen from the RCA trunk, excluding the RCA-PDA, in control right ventricles and 23 RCA-RVB in hypertrophic right ventricles is shown in Fig. 5.

Tables 2 and 3 show the mean diameters and lengths of vessel segments and elements in each order of vessels in the right ventricular branches of the RCA of control and hypertrophic right ventricles, respectively. A segment is a vessel between two successive nodes of bifurcation, whereas an element is a combination of segments of the same order in series. These tables show that a total of 10 and 11 orders of vessels lie between the coronary capillaries and the largest right ventricular branches for the control and hypertrophic right ventricles, respectively.

Figure 6 shows the relationship between the mean vessel diameter and the order number for the elements of the RCA-RVB in control and hypertrophic right ventricles, respectively. Figure 7 shows the relationship between the

Table 1. *Hemodynamic data and morphometric specimens from control and hypertrophic pig RV*

Pig	Weight, g			Blood Pressure, mmHg		Morphometry From	
	RV	RV/LV	Perfused RV	RV	Aorta	Histology	Cast
				Control RV			
A	21.1	0.29	12.5	23/3	130/105	Yes	Yes
B	18.5	0.29	14.8	26/1	110/90	Yes	No
				Hypertrophic RV			
C	52.3	0.67	41.9	95/0	165/120	Yes	Yes
D	58.7	0.63	30.5	73/0	105/85	Yes	No
E	61.0	0.69	44.8	60/0	130/90	Yes	No

Blood pressure values are systolic/diastolic. LV and RV, left and right ventricles, respectively.

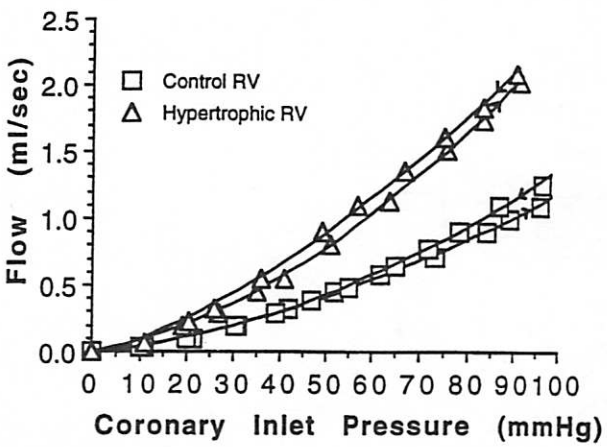

Fig. 4. Pressure-flow relation of RCA in control and hypertrophic pig RV.

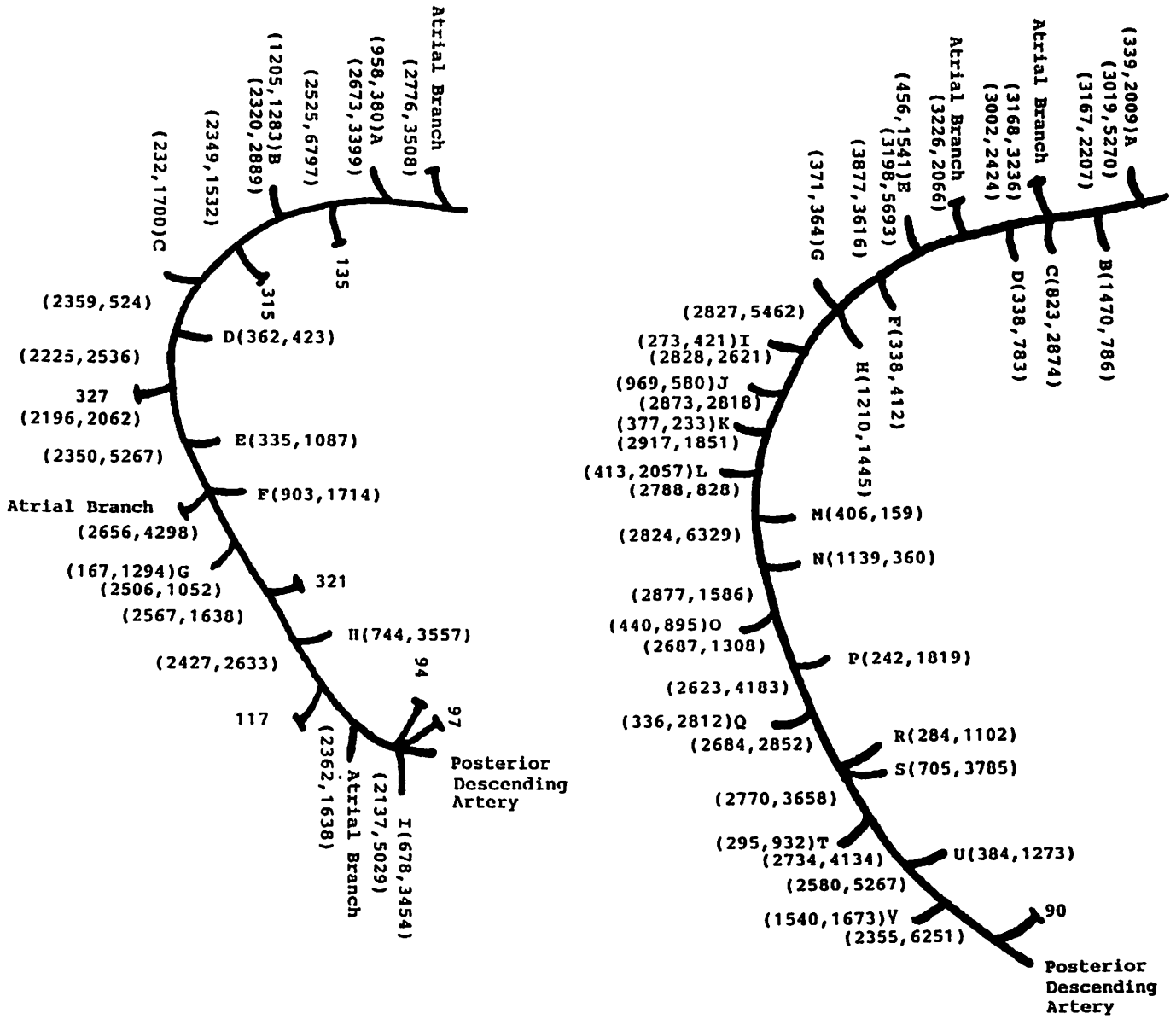

Fig. 5. Sketches of RCAs marked with measured diameters and lengths (in μm) of vessel segments in control and hypertrophic pig RV.

Table 2. *Diameters and lengths of vessel segments and elements in each order of vessels in control pig RV arterial branches*

Order	Segments				Elements			
	Diameter, μm	*n*	Length, mm	*n*	Diameter, μm	*n*	Length, mm	*n*
1	9.7±0.95	823	0.073±0.048	383	9.5±0.84	99	0.138±0.092	99
2	13.6±1.5	599	0.083±0.055	348	13.4±1.1	95	0.149±0.115	95
3	19.8±2.4	398	0.087±0.062	266	18.8±1.7	52	0.172±0.103	52
4	30.1±4.5	767	0.180±0.170	343	29.8±3.6	60	0.332±0.210	60
5	59.8±9.2	533	0.368±0.311	313	49.5±6.5	50	1.23±0.800	50
6	102±20.9	441	0.601±0.461	347	97.0±13.9	46	2.24±1.20	46
7	201±36.9	203	0.723±0.625	192	191±26.3	47	2.55±1.88	47
8	385±70.8	76	1.11±0.804	70	370±53.2	11	5.18±4.65	11
9	701±126	53	1.47±1.07	52	669±45.0	5	11.9±6.71	5
10	1,016±107	10	2.25±0.995	10	1,007	2	9.62	2

Values are means ± SD; *n*, no. of vessels measured.

Table 3. *Diameters and lengths of vessel segments and elements of each order of RV arterial branches of RV hypertrophic pig*

Order	Segments				Elements			
	Diameter, μm	*n*	Length, mm	*n*	Diameter, μm	*n*	Length, mm	*n*
1	9.7±1.0	865	0.071±0.051	353	9.5±0.92	148	0.105±0.084	148
2	13.2±1.2	803	0.074±0.051	416	13.0±1.2	176	0.137±0.10	176
3	17.9±1.6	616	0.081±0.061	402	17.7±1.5	162	0.174±0.14	162
4	25.9±3.0	1,881	0.170±0.17	446	25.3±3.1	157	0.237±0.18	157
5	40.0±5.5	2,063	0.342±0.28	794	39.6±5.1	259	0.546±0.39	259
6	65.6±11.0	2,428	0.457±0.36	1,603	65.4±9.6	387	1.07±0.76	387
7	121±23.1	1,294	0.576±0.47	1,238	124±19.7	250	2.15±1.41	250
8	224±37.0	562	0.707±0.53	544	238±27.8	109	2.82±1.92	109
9	396±79.2	212	1.00±0.77	203	404±57.4	40	4.29±3.94	40
10	837±175	100	1.54±1.10	98	881±126	7	16.6±10.7	7
11	1,350±122	22	2.50±2.03	22	1,325	2	16.3	2

Values are means ± SD; *n*, no. of vessels measured.

mean vessel element length and the order number for the RCA-RVB in control and hypertrophic right ventricles, respectively. The curves in Fig. 6 obey Horton's law (13, 16). The ratio of the diameters of successive orders of arteries is a constant independent of *n* and is called the "diameter ratio." The diameter ratio is given by the antilog of the slope of the lines of Fig. 6. The mean element length also obeys Horton's law but with a discontinuity in the slope at order 3 (Fig. 7). The mean element diameter

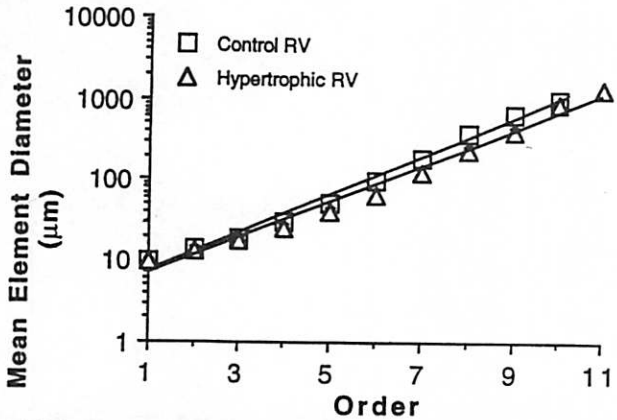

Fig. 6. Relation between average diameters of vessel elements in successive orders of vessels and order number of vessels in RV branches (RCA-RVB) of control and hypertrophic pig RV.

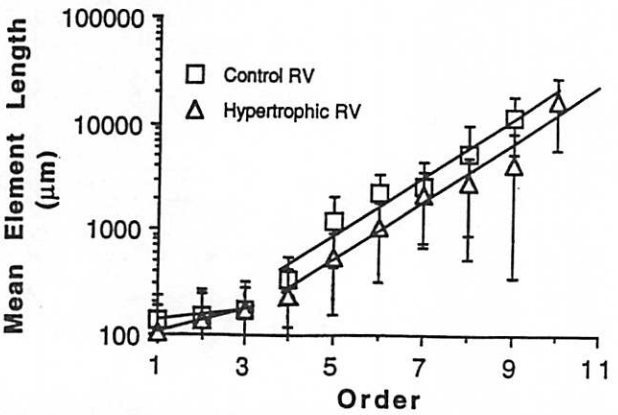

Fig. 7. Relation between average lengths of vessel elements in successive orders of vessels and order number of vessels in RCA-RVB of control and hypertrophic pig RV.

ratios of RCA-RVB in control and hypertrophic right ventricles are 1.73 and 1.67, respectively, whereas the mean element length ratios of RCA-RVB in control and hypertrophic ventricles are 1.89 and 1.89, respectively, for orders 4–10 but are 1.12 and 1.29, respectively, for orders 1–3.

The ratio of the segment number and the element number (S/E) is presented in Table 4. It can be plotted as a function of *n* for each tree and fitted by a fourth-order polynomial. The fitting is shown in Fig. 8. The S/E ratio has the physical meaning of the average number of vessel segments in series. The largest orders are most asymmetric. The degree of asymmetry decreases with a decrease in the order number in control and hypertrophic right ventricles.

The connectivity matrices of the RCA-RVB in control and hypertrophic right ventricles are given in Tables 5 and 6, respectively. The total number of arterial elements of each order can be computed from information on the number of intact and cut elements and the connectivity matrix as illustrated in the APPENDIX of our companion report (16). Similar analysis is carried out for each RCA-RVB, whose location along the RCA trunk is shown in Fig. 5. The total number of elements is then summed over all RCA-RVB trees at each order to give the total number

Table 4. *S/E for each order of vessels in RV arterial branches of control and RV hypertrophic pig*

Order	Control RV		Hypertrophic RV	
	S/E	*n*	S/E	*n*
1	1.93±0.99	101	1.55±0.87	148
2	1.92±1.0	95	1.78±0.95	176
3	2.08±1.1	60	1.96±1.2	162
4	2.10±1.6	60	1.36±0.76	157
5	3.20±1.9	50	1.54±0.81	259
6	3.83±2.3	46	2.25±1.3	387
7	3.57±2.9	47	3.80±2.5	250
8	5.18±5.0	11	3.74±3.1	109
9	8.20±4.1	5	3.98±3.4	40
10	5.5	2	7.86±5.9	7
11			7.0	2

Values are means ± SD; *n*, no. of observations. S/E, segment-to-element numbers ratio, which is ratio of total no. of segments in a given order to total no. of elements in that order.

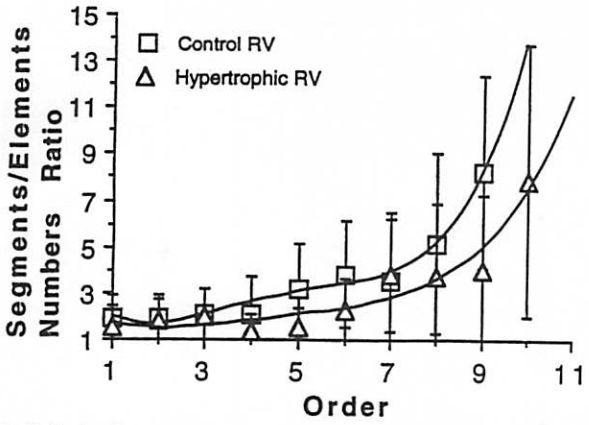

Fig. 8. Relation between average number of segments in series in successive orders of vessels and order number of vessels in RCA-RVB of control and hypertrophic pig RV.

of elements at that order. The results, means ± propagated errors, are presented in Table 7. If the total number of arterial segments of each order is desired, one need only to multiply the number of elements by the ratio of the number of segments to the number of elements presented in Table 4.

When the number of elements of order n is normalized with respect to the perfused myocardial mass given in Table 1 and plotted against n on a semilog paper (Fig. 9), the data fit a straight line. Thus the number of vessels increases as an inverse geometric sequence in accordance with Horton's law (13). The ratio of the numbers of vessels of successive orders is a constant independent of n and is called the "branching ratio." The branching ratio is given by the antilog of the absolute value of the slope of the lines of Fig. 9. The element branching ratios of RCA-RVB in control and hypertrophic right ventricles are 3.13 and 2.98, respectively.

The data on the diameters, lengths, and number of elements are used to compute the total CSAs and blood volumes, as shown previously (16). The total CSAs are normalized with respect to the perfused myocardial mass given in Table 1, plotted in Fig. 10, and fitted with fifth-order polynomials by the least-squares method. Similarly, the total blood volumes in all elements of a given order are normalized with respect to the perfused myocardial mass and are shown in Fig. 11.

DISCUSSION

We experimentally determined the resistance of the RCA in control and hypertrophic right ventricles by measuring their P-$\dot{Q}$ relationships in the isolated heart preparation, as shown in Fig. 4. The inverse of the slope of these curves represents the total resistance to flow of the

Table 5. *Connectivity matrix for RV arterial branches of control pig*

Order n	Order m									
	1	2	3	4	5	6	7	8	9	10
0	2.84±0.101	0.642±0.085	0.133±0.041	0.017±0.017	0	0	0	0	0	0
1	0.099±0.030	2.22±0.081	0.800±0.108	0.233±0.069	0.520±0.050	0.174±0.056	0.170±0.076	0	0	0
2		0.063±0.029	2.13±0.084	1.10±0.157	0.580±0.111	0.522±0.131	0.213±0.067	0.273±0.195	0	0
3			0.033±0.023	1.65±0.091	1.14±0.183	0.630±0.105	0.511±0.128	0.364±0.152	0.600±0.245	0
4				0.167±0.048	1.96±0.148	1.11±0.159	1.00±0.182	1.09±0.494	0.400±0.245	0
5					0.200±0.057	2.33±0.143	1.17±0.170	1.27±0.573	2.00±0.707	1.0
6						0.152±0.053	1.81±0.138	1.73±0.604	3.40±0.927	1.0
7							0.064±0.036	2.09±0.342	2.20±0.860	0.50
8								0	1.40±0.245	2.5
9									0	1.5
10										0

Values are means ± SE. An element (m,n) in mth row and nth column is ratio of total no. of elements of order m that spring directly from parent elements of order n divided by total no. of elements of order n.

Table 6. *Connectivity matrix for RV arterial branches of RV hypertrophic pig*

Order n	Order m										
	1	2	3	4	5	6	7	8	9	10	11
0	2.55±0.075	0.608±0.066	0.426±0.077	0.013±0.009	0	0	0	0	0	0	0
1	0.041±0.023	2.14±0.076	0.660±0.066	0.115±0.029	0.077±0.017	0.049±0.014	0.060±0.017	0.055±0.02	0	0	0
2		0.057±0.017	2.03±0.072	0.650±0.059	0.309±0.038	0.181±0.025	0.128±0.023	0.064±0.030	0.125±0.053	0	0
3			0.099±0.031	1.61±0.065	0.741±0.049	0.411±0.032	0.404±0.047	0.257±0.069	0.125±0.064	0.143±0.143	0
4				0.025±0.016	1.39±0.045	0.755±0.046	0.692±0.061	0.404±0.067	0.575±0.179	0.286±0.286	0.50
5					0.042±0.014	1.80±0.044	1.05±0.074	0.945±0.121	0.875±0.172	0.714±0.286	1.0
6						0.109±0.017	2.50±0.080	1.39±0.127	1.08±0.228	2.86±0.705	3.5
7							0.180±0.027	2.05±0.103	0.850±0.195	1.86±0.705	3.5
8								0.073±0.025	1.92±0.166	3.71±1.27	1.0
9									0.050±0.035	3.57±1.27	1.0
10										0	2.0
11											0

Values are means ± SE. An element (m,n) in mth row and nth column is ratio of total no. of elements of order m that spring directly from parent elements of order n divided by total no. of elements of order n.

Table 7. *Total number of vessel elements in each order of RV arterial branches of control and RV hypertrophic pig*

Order	Number of Vessel Elements	
	Control RV	Hypertrophic RV
11		2
10	2	11
9	7	60±3
8	22±1	180±15
7	82±16	626±66
6	271±96	2,369±301
5	1,021±418	5,749±868
4	3,039±1,535	10,960±2,077
3	6,676±3,838	25,963±6,670
2	19,608±12,705	66,086±20,280
1	55,720±40,093	167,335±61,689

Values are means ± SE, expressed in no. of vessel elements.

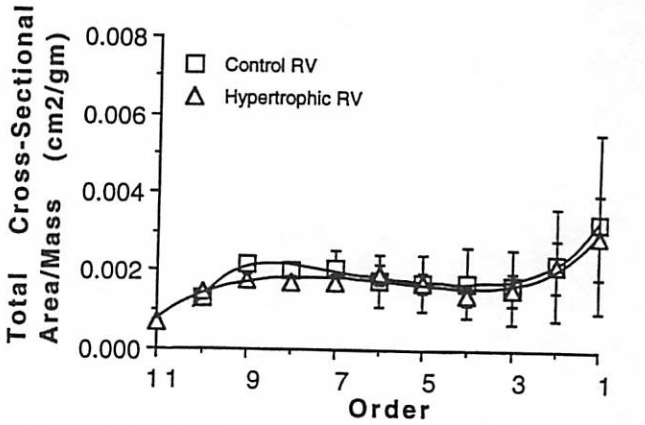

Fig. 10. Relation between calculated total cross-sectional area of arterial branches in each order and order number for RCA-RVB of control and hypertrophic pig RV.

RCA circuit. We found that the flow (volume/time) resistance through the RCA decreased in RVH (Fig. 4).

The diameter of the trunk of the RCA increased with RVH. The diameters of the RCA-RVB arising from the RCA also increased (Figs. 3 and 5). The length of the trunk, which crowns the base of the heart, increased in RVH. The number of RCA-RVB arising from the trunk also increased in RVH. These results are consistent with the angiogenesis described by White et al. (32) in which a moderate DNA synthesis was found in smooth muscle cells.

The mean diameters of the vessel segments and elements were slightly smaller, at each order, in RVH (Fig. 6). Progressing from the smallest arteriole to the largest RCA-RVB in the hypertrophied right ventricle required 11 orders. In contrast, this progress in the control right ventricle required only 10 orders. This reflects both the increased diameter of the largest RCA-RVB in RVH and the remodeling of the branching patterns of the RCA arterial circuit. The remodeling of the branching patterns is best seen in S/E (Fig. 8). The RVH arterial trees are more symmetrical at any order than those of the corresponding control hearts. The segment and element lengths are decreased in RVH (Fig. 7). Angiogenesis of arterioles, active DNA synthesis, in this RVH model in the early stages of hypertrophy was previously demonstrated with tritiated thymidine labeling (34). Angiogenesis in RVH contributed to the increased number of vessels (Fig. 9). However, the increase in the number of small arterioles is most important, since those arterioles are the major sites of vascular resistance (8, 14, 28).

The total CSA of the RCA-RVB is larger in hypertrophic than control right ventricles. This increase in CSA is due to the large increase in the number of parallel elements. However, the CSA-to-mass ratio of RCA-RVB is similar in both control and hypertrophic right ventricles (Fig. 10). The volume of the RCA-RVB is also larger in RVH. Again, when we normalize the volume of the RCA-RVB for the mass perfused, we find some compensation (Fig. 11). The mass-normalized accumulative volume decreases 11% in RVH. In conclusion, the RCA-RVB appears to adapt in the hypertrophic right ventricle through compensatory vascular growth and remodeling.

Studies by Breisch et al. (6, 7) and Tomanek et al. (30) have shown that left ventricles subjected to pressure overload that induces ventricular hypertrophy of >50% have increased total coronary perfusion even though minimal coronary resistance increases. Furthermore, this increase in total flow correlated with increased numbers and CSAs of small arterioles, showing that angiogenesis can occur in the left ventricle subjected to pressure overload. Thus

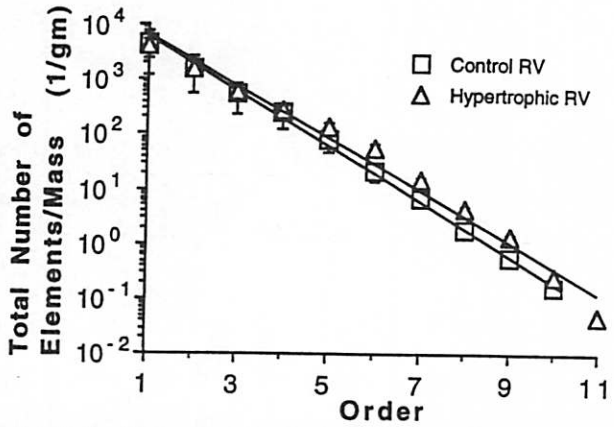

Fig. 9. Relation between total corrected number of parallel elements in successive orders of vessels and order number of vessels in RCA-RVB of control and hypertrophic pig RV.

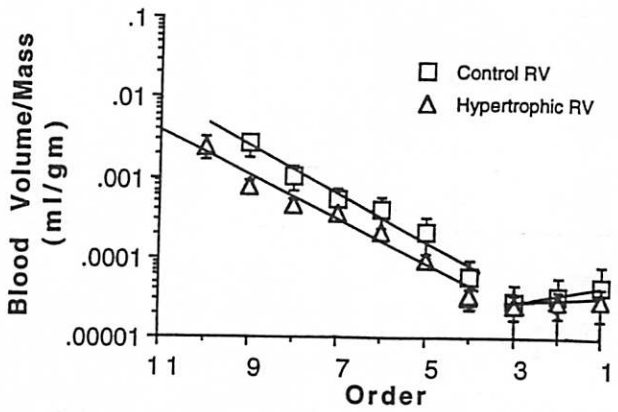

Fig. 11. Relation between calculated total blood volume of arterial branches in each order and order number for RCA-RVB of control and hypertrophic pig RV.

pressure-overload hypertrophy can stimulate angiogenesis, and the maintenance of minimal coronary resistance occurs by the growth of small arterioles.

Studies of coronary vascular adaptations occurring in pressure overload-induced LVH agree that there is a decrease in coronary blood flow reserve primarily due to inadequate vascular growth with a smaller vascular CSA than control (3, 6, 9, 23, 29, 34). It should be noted that these vascular adaptations occur in a setting where isolated pressure overload is imposed on the left ventricle. When LVH is induced by other means (e.g., renal, systemic, or genetic hypertension), the changes may differ, since other nonpressure factors are introduced in those settings.

In contrast, the right ventricle is much less susceptible to decreases in coronary blood flow reserve when the ventricle is stressed (5, 10, 17–20). These studies suggest that an increase in vascular CSA occurs that maintains blood flow reserve at control levels as the myocytes enlarge. An exception to this is the study by Vatner (31), in which the dog model right ventricular coronary blood flow decreased compared with control during reactive hyperemia or during maximal vasodilation. However, Botham et al. (5) have shown that, in puppies with banding of the pulmonary artery, there is an increase in coronary blood flow reserve, suggesting an increase in vascular CSA. Because these dogs were in an active growth phase as RVH progressed, angiogenesis was probably more pronounced. Our pigs were young adults. Although their active growth phase should be reaching a plateau, the level of growth hormone could play a key role in the vascular compensation observed in progressive RVH. Recently Dobbs et al. (11) showed that coronary collateral development after the onset of ischemia was similar in pigs of varying ages, ranging from 4 mo to 3 yr. This suggests that coronary vascular adaptations, especially neovascularization and angiogenesis, are uniform unless the subjects are very young, in an active growth phase, or older, when other pathological changes may also be present.

Previously (32) we showed that resistance to blood flow in the right coronary arterial vascular bed changes during progressive RVH. Our results showed that hypertrophic right ventricles have decreased diameters and lengths at each order of vessels in the RCA-RVB vascular bed. There is also a one-order increase in the total number of orders in the hypertrophic right ventricle (from 10 orders in the control to 11 orders in RVH). Total RCA arterial resistance decreased in RVH due to increases in total CSAs of each order of vessel and the number of parallel vessel elements within each order. Our P-$\dot{Q}$ curves from isolated heart preparations obtained from these models showed coronary resistance decreases in RVH that correlated with the morphometric findings. We conclude that there is significant remodeling of the coronary arterial vasculature in the hypertrophic right ventricle. Future analysis of coronary circulation of hypertrophic right ventricle must take into account the morphometric remodeling.

This research is supported by National Heart, Lung, and Blood Institute Training Grants HL-07089, HL-43026, and HL-20190; the American Heart Association, California Affiliate, through Postdoctoral Fellowship 90-51 (to G. S. Kassab); and US National Science Foundation Grant BCS-89-17576.

Address for reprint requests: C. M. Bloor, Dept. of Pathology, UCSD School of Medicine, 9500 Gilman Dr., La Jolla, CA 92093-0612.

Received 14 February 1992; accepted in final form 18 February 1993.

REFERENCES

1. **Anversa, P., P. C. Beghi, V. Levicky, S. L. McDonald, and Y. Kikkawa.** Morphometry of right ventricular hypertrophy induced by strenuous exercise in the rat. *Am. J. Physiol.* 243 (*Heart Circ. Physiol.* 12): H856–H861, 1982.
2. **Anversa, P., and J. M. Capasso.** Loss of intermediate-sized coronary arteries and capillary proliferation after left ventricular failure in rats. *Am. J. Physiol.* 260 (*Heart Circ. Physiol.* 29): H1552–H1560, 1991.
3. **Bache, R. J., X.-Z. Dai, D. Alyono, T. R. Vrobel, and D. C. Homann.** Myocardial blood flow during exercise in dogs with left ventricular hypertrophy produced by aortic banding and perinephritic hypertension. *Circulation* 76: 835–842, 1987.
4. **Bache, R. J., T. R. Vrobel, C. E. Arentzen, and W. S. Ring.** Effect of maximal coronary vasodilation on transmural myocardial perfusion during tachycardia in dogs with left ventricular hypertrophy. *Circ. Res.* 49: 742–750, 1981.
5. **Botham, M. J., J. H. Lemmer, R. A. Gerren, R. W. Long, D. M. Behrendt, and K. P. Gallager.** Coronary vasodilator reserve in young dogs with moderate right ventricular hypertrophy. *Ann. Thorac. Surg.* 38: 101–107, 1984.
6. **Breisch, E. A., F. C. White, and C. M. Bloor.** Myocardial characteristics of pressure overload hypertrophy: a structural and functional study. *Lab. Invest.* 51: 333–342, 1984.
7. **Breisch, E. A., F. C. White, L. E. Nimmo, M. D. McKirnan, and C. M. Bloor.** Exercise-induced cardiac hypertrophy: a correlation of blood flow and microvasculature. *J. Appl. Physiol.* 60: 1259–1267, 1986.
8. **Chilian, W. M., C. L. Eastham, and M. L. Marcus.** Microvascular distribution of coronary vascular resistance in beating left ventricle. *Am. J. Physiol.* 251 (*Heart Circ. Physiol.* 20): H779–H788, 1986.
9. **Cimini, C. M., and H. R. Weiss** Microvascular morphometry and perfusion in renal hypertension-induced cardiac hypertrophy. *Am. J. Physiol.* 255 (*Heart Circ. Physiol.* 24): H1384–H1390, 1988.
10. **Cooper, G., R. J. Tomanek, J. C. Ehrhardt, and M. L. Marcus.** Chronic progressive pressure overload of the cat right ventricle. *Circ. Res.* 48: 488–497, 1981.
11. **Dobbs, S. L., D. M. Roth, C. M. Bloor, and F. C. White.** Effects of age on coronary collateral development. *Coronary Artery Dis.* 2: 473–480, 1991.
12. **Hoffmann, J. I. E.** A critical view of coronary reserve. *Circulation* 75, *Suppl.* I: I-6–I-11, 1987.
13. **Horton, R. E.** Erosional development of streams and their drainage basins: hydrophysical approach to quantitative morphology. *Bull. Geol. Soc. Amer.* 56: 275–370, 1945.
14. **Kanatsuka, H., K. G. Lamping, C. L. Eastham, M. L. Marcus, and K. C. Dellsperger.** Coronary microvascular resistance in hypertensive cats. *Circ. Res.* 68: 726–733, 1991.
15. **Kassab, G. S.** *Morphometry of the Coronary Arteries in the Pig* (PhD thesis). La Jolla: Univ. of California, San Diego, 1990.
16. **Kassab, G. S., C. A. Rider, N. J. Tang, and Y. C. Fung.** Morphometry of pig coronary arterial trees. *Am. J. Physiol.* 265 (*Heart Circ. Physiol.* 34): H350–H365, 1993.
17. **Manohar, M.** Transmural coronary vasodilator reserve and flow distribution during tachycardia in conscious young swine with right ventricular hypertrophy. *Cardiovasc. Res.* 19: 104–112, 1985.
18. **Manohar, M., G. E. Biscard, V. Bullard, and J. H. Rankin.** Blood flow in the hypertrophied right ventricular myocardium of unanesthetized ponies. *Am. J. Physiol.* 240 (*Heart Circ. Physiol.* 9): H881–H888, 1981.
19. **Manohar, M., G. E. Bisgard, V. Bullard, J. A. Will, D. Anderson, and J. H. G. Rankin.** Regional myocardial blood flow and myocardial function during acute right ventricular pressure overload in calves. *Circ. Res.* 44: 531–539, 1979.
20. **Manohar, M., J. C. Thurmon, W. J. Tranquilli, M. D. Devous, M. C. Theodorakis, R. V. Shawley, D. L. Feller, and G. J. Benson.** Regional myocardial blood flow and coronary vascular reserve in unanesthetized calves with severe concentric right ventricular hypertrophy. *Circ. Res.* 48: 785–787, 1981.

21. **Marcus, M. L., T. M. Mueller, J. A. Gascho, and R. E. Kerber.** Effects of cardiac hypertrophy secondary to hypertension on the coronary circulation. *Am. J. Cardiol.* 44: 1023–1028, 1979.
22. **Murry, P. A., H. Baig, M. C. Fishbein, S. F. Vatner.** Effects of experimental right ventricular hypertrophy on myocardial blood flow in conscious dogs. *J. Clin. Invest.* 64: 421–427, 1979.
23. **O'Keefe, D. D., J. I. E. Hoffmann, R. Cheitlin, M. J. O'Neill, J. R. Allard, and E. Shapkin.** Coronary blood flow in experimental canine left ventricular hypertrophy. *Circ. Res.* 43: 43–51, 1978.
24. **Olivetti, G., R. Ricci, C. Lagraste, E. Maniga, E. Sonneblick, and P. Anversa.** Cellular basis of wall remodeling in longterm pressure overload induced right ventricular hypertrophy in rats. *Circ. Res.* 63: 648–657, 1988.
25. **Rakusan, K.** Quantitative morphology of capillaries of the heart. Number of capillaries in animal and human hearts under normal and pathological conditions. *Methods Achiev. Exp. Pathol.* 5: 272–285, 1971.
26. **Rakusan, K.** Microcirculation in the stressed heart. In: *The Stressed Heart*, edited by M. J. Legato. Boston, MA: Nijhoff, 1987, p. 107–123.
27. **Rakusan, K., and P. Wicker.** Morphometry of the small arteries and arterioles in the rat heart: effects of chronic hypertension and exercise. *Cardiovasc. Res.* 24: 278–284, 1990.
28. **Tillmanns, H., M. Steinhausen, H. Leinberger, H. Thederan, and W. Kubler.** Pressure measurements in the terminal vascular bed of the epimyocardium of rats and cats. *Circ. Res.* 49: 1202–1211, 1981.
29. **Tomanek, R. J., P. J. Palmer, G. L. Peiffer, K. L. Schreiber, C. L. Eastham, and M. L. Marcus.** Morphometry of canine coronary arteries, arterioles, and capillaries during hypertension and left ventricular hypertrophy. *Circ. Res.* 58: 38–46, 1986.
30. **Tomanek, R. J., K. A. Schalk, M. L. Marcus, and D. G. Harrison.** Coronary angiogenesis during long-term hypertension and left ventricular hypertrophy in dogs. *Circ. Res.* 65: 352–359, 1989.
31. **Vatner, S. F.** Reduced subendocardial myocardial perfusion as one mechanism for congestive heart failure. *Am. J. Cardiol.* 62: 94E–98E, 1988.
32. **White, F., Y. Nakatani, L. Nimmo, and C. Bloor.** Compensatory angiogenesis in compensated, progressive right ventricular hypertrophy. *Am. J. Cardiovasc. Pathol.* 4: 46–61, 1992.
33. **White, F. C., M. D. McKirnan, E. A. Breisch, B. D. Guth, Y. M. Liu, and C. M. Bloor.** Adaptation of the left ventricle to exercise-induced hypertrophy. *J. Appl. Physiol.* 62: 1097–1110, 1987.
34. **White, F. C., T. M. Sanders, T. Peterson, and C. M. Bloor.** Ischemic myocardial injury after exercised stress in the pressure overloaded heart. *Am. J. Pathol.* 97: 473–488, 1979.